



Since January 2020 Elsevier has created a COVID-19 resource centre with free information in English and Mandarin on the novel coronavirus COVID-19. The COVID-19 resource centre is hosted on Elsevier Connect, the company's public news and information website.

Elsevier hereby grants permission to make all its COVID-19-related research that is available on the COVID-19 resource centre - including this research content - immediately available in PubMed Central and other publicly funded repositories, such as the WHO COVID database with rights for unrestricted research re-use and analyses in any form or by any means with acknowledgement of the original source. These permissions are granted for free by Elsevier for as long as the COVID-19 resource centre remains active.

V CIRP Conference on Biomanufacturing

Technological scouting of bi-material face masks: simulation of adherence using 3D Facial Norms

Elisa Ficarella^{a*}, Angelo Natalicchio^a, Roberto Spina^a, Luigi Maria Galantucci^a

^aPolitecnico di Bari, Via Edoardo Orabona 4, 70126, Bari, Italy

* Corresponding author. Tel.: +39 339 219 1669. E-mail address: elisa.ficarella@poliba.it

Abstract

During the COVID-19 pandemic started in March 2020, the need for personal protective equipment rapidly grew as it became mandatory. The availability of a set of faces can be of great utility in designing a face mask with proper adherence and comfortability in wearing and breathing. A 3D geometry of a face with user-defined anthropometric measures was generated with Blender, a powerful development tool for creating 3D images. Using 3D Facial Norms, a free online database, it was possible to compute the mean anthropometric measures for the age groups of 17-20, 20-30, and 30-40 years old and then generate the respective faces for both genders. The adherence of an innovative face mask was then simulated with the reverse engineering software considering both the face mask and the faces rigid.

© 2022 The Authors. Published by Elsevier B.V.

This is an open access article under the CC BY-NC-ND license (<https://creativecommons.org/licenses/by-nc-nd/4.0>)

Peer-review under responsibility of the scientific committee of the V CIRP Conference on Biomanufacturing

Keywords: face masks; parametric face; COVID-19

1. Introduction

1.1. Covid-19 pandemic

The COVID-19 pandemic, declared by the World Health Organization (WHO) in March 2020, highlighted the fragility and vulnerability of conventional global supply chains. The auto-isolation of China, a worldwide supplier of raw or semi-processed material in many fields, led to a shortage in the supply of medical and non-medical products, including personal protective equipment (PPE) [1–3].

During this pandemic, Governments and WHO advised the population to use masks to reduce the diffusion of COVID-19, such as cloth masks (cotton or gauze), medical masks (medical, surgical, or procedural), and respirators (N95, N99, N100, P2, P3, FFP2, and FFP3) [4–6], which were well-fitted devices designed to protect from respiratory infections, arranged according to their filtration capacities [7].

Face masks now have a well-established role in mitigating the spread of COVID-19, preventing symptomatic and

asymptomatic transmission [2,3,8]. Face masks are highly requested worldwide as a healthcare necessity, and billions are produced. These face masks are constituted of petrochemical-derived raw materials, which are non-degradable or reusable, thus affecting and damaging the environment [9]. Concerning materials, disposable masks were made using several polymers such as polyethylene, polycarbonate, and polyester. Synthetic polymers such as polypropylene, polystyrene, polylactic acid, and polyethylene terephthalate were applied to design and fabricate face mask shields, although natural polymers could be a valid substitute for synthetic polymers [10].

Another problem caused by the massive use of face masks, especially for health workers, is the comfort of wearing them. Surgical masks and more FFP2/N95 face masks cause discomfort and reduce ventilation and cardiopulmonary exercise capacity [11]. FFP2/N95 adheres better on the face, causing more discomfort and providing more filtering action [12]. It is essential for face masks to adhere the best to the face to provide the necessary protection [13].

Considering all the above aspects, locally producing a comfortable, breathing, and sustainable mask is highly necessary.

1.2. RIAPRO at Politecnico di Bari

During the outbreak of the COVID-19 pandemic, in March 2020, Politecnico di Bari launched a project named R.I.A.PRO (RIconversione Aziendale per la PROduzione di DPI, literally *Corporate reconversion for the PPE production*), supported by the Apulia Region (Italy), in coordination with the other regional universities. This project was a helpful tool and reference for small and medium-sized enterprises located in Apulia and other Italian regions to undertake a conversion process to produce medical and anti-COVID-19 products [14].

The Apulian company, New Euroart S.r.l. in Grumo Appula (Bari, Italy), realized an innovative, comfortable product named Lala Mask[®]. This product is fully sanitizable and washable with soaps and alcohol, hypoallergenic and recyclable; it aims to guarantee facial adherence, lightness, and high breathability [15,16]. The mask consisted of two different polymers chemically joined during a sequential injection molding process. The rigid part of the mask, called *body*, was made in Polypropylene (PP), while the flexible part in contact with the body skin, called *rubber*, was made in Thermoplastic Elastomer (TPE). All materials were of medical grades.

1.3. 3D printing for face masks

Under the outbreak of COVID-19, 3D printing technology helped overcome shortages of critical supplies [17–19]. Recent studies proposed alternative 3D printing processes and materials [3]. This unregulated supply chain opened up new medical certification and intellectual property rights [20]. Other initiatives consisted of several open-source files of 3D printable masks available on platforms or websites of companies operating in the 3D printing sector. The open-source *MY FACE MASK Add-on* for Blender [21], a free and open-source 3D creation suite, generated a custom mask modeled from a 3D scan of the human face. Masks generated with this add-on were also suitable for 3D printing [22]. Using this add-on, the face area where the mask adhered was identified with a brush. The 3D model of the template was finally exported in STL format, ready for production.

1.4. Description of an innovative mask

A patent analysis was performed to understand the technological scenario to design and manufacture the face masks, analyzing the opportunity to develop an innovative face mask. Therefore, a search string¹ to collect relevant patents for

the analysis was defined, and the Orbit² database was used to retrieve the patents to be successively analyzed³. The search was carried out on patent titles, abstracts, and claims to obtain relevant results and avoid potential “false positives” without limiting the exploration to a specific time interval. After the search, the patents retrieved were scrutinized to remove irrelevant results. A final group of 147 patents was achieved, corresponding to 92 patent families⁴ and related data. By analyzing the first application date for each family, the patented technologies applied between 1989 and 2021 were spotted (see Fig. 1). A dramatic rise in applications in 2020 was discovered, probably related to the outbreak of the COVID-19 pandemic.

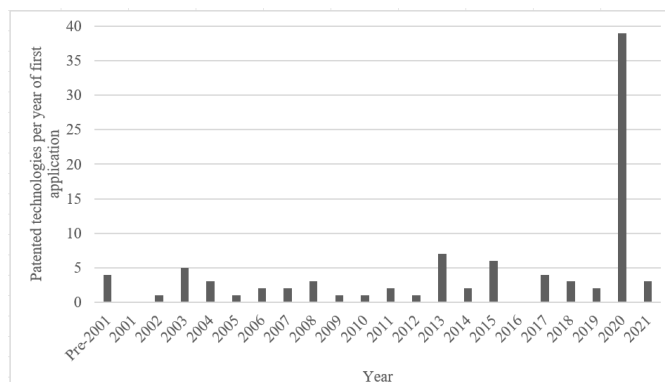


Fig. 1. Number of patented technologies filed per year

Concerning the offices where the retrieved patents were registered, the leading one was the Chinese patent office with 75 patents, followed by the South Korean (9 patents), Japanese (8 patents), and United States (6). Data suggested that Chinese firms and individuals were the leading ones regarding patented technologies owned, indicating a lively innovative activity on face masks in China.

To evaluate the relevance of the face mask patents collected for the analysis, forward citations from each family of patented technology were relied on. Indeed, forward citations indicate the influence of patented technology on subsequent developments. Henceforward citations were widely used in the patent literature to assess patents' technological and economic value [23–25]. However, to avoid time-related effects that could potentially bias the analysis, the number of forwarding citations received by each family of patented technology was divided by the patent age, calculated as the number of years elapsed since the first application of the focal technology [26]. The analysis based on this indicator showed that the five most impactful technologies (i.e., the patented technologies with the highest value of forwarding citations per year) are the following:

¹ The search string used for the patent retrieval was: ((mask AND face) OR (facemask)) AND (virus) AND (filter) AND (fit OR comfortability OR wear). This string allowed to concurrently consider the object of invention (i.e., the face mask), its protection function, and its comfortability, hence covering all the relevant aspect for the development of an ergonomic face mask to protect humans against viruses, such as the COVID-19 one.

² Orbit Intelligence is a database developed by Questel containing data on more than 100 million patents registered in worldwide patent offices, thus providing a complete source of information for our analysis.

³ The search for patents was performed at the beginning of June 2021.

⁴ Patent families are groups of patents protecting an invention in more than one patent office [39].

- *Virucidal material* (first publication GB0603138 in 2006, 3.8 citations/year): a material to produce protective clothing for face mask manufacturing, avoiding virus transmission.
- *Devices for decreasing human pathogen transmission* (first publication WO2009/003057 in 2008, 2.4 citations/year): a face mask to avoid virus transmission, endowed with a fabric layer to attach human pathogens chemically.
- *Ultra-thin polymer film and porous ultra-thin polymer film* (first publication WO2013/137260 in 2013, 2.1 citations/year): a method to produce an ultra-thin polymer film to prevent the passage of microorganisms.
- *Face mask for the protection against biological agents* (first publication ITPS20040007 in 2004, 1.8 citations/year): a face mask endowed with a filtering layer, a high-efficiency exhalation valve, and a boundary sealing layer to favor the sealing between mask and face.
- *Positive-pressure protective clothing with virus prevention, purification, ventilation, exhaust, and heat dissipation* (first publication CN111135493 in 2020, 1 citation/year): clothing comprising a head-mounted protective mask to prevent virus transmission for ventilation and heat dissipation.

This analysis showed that impactful patents were mainly focused on virus prevention, while the wearability and the comfortability of face masks was an aspect relatively neglected or that existing technologies did not effectively satisfy. The analysis also indicated a technological gap to fill by introducing a new face mask offering protection and comfort to people wearing it.

2. Modeling of faces and evaluation of geometrical adherence

2.1. Identification of characteristic anthropometrics measures

Literature analysis for anthropometric facial measurements was performed to evaluate the adherence of a mask to the human face. A *reference face* covering the anatomical characteristics of most users was defined. Anthropometric facial measurements were evaluated by computing the distances among standardized anatomical points. This work considered a collection of the central line and lateral landmarks acquired using a 3D photogrammetric methodology developed by the authors [27–29]. The online 3DFN (3D Facial Norms) database was used due to its valuable and complete availability of anatomical facial measurements made with 3D stereophotogrammetry. The database consisted of 2,454 individuals from 3 to 40 years old who belonged to the Caucasian European genome. Anthropometric measurements evaluated the distance between facial landmarks (e.g., *nasion*, *gnation*) from 3D images. The database also provided statistical measurements according to gender and age [30].

The faces for assessing the mask adaptability were selected considering:

- Two genders (Male and Female).
- Three age groups: 17–20, 21–30, 31–40 years old, corresponding to puberty, youth, and maturity, respectively.

The maximum age of 40 was set because no data beyond this age was available. However, a defined trend in anthropometric measurements was identified by analyzing the graphs (Fig. 2). The values could be extrapolated for other age groups such as 40–50 and 50–60 years old. By combining typology, gender, and age group, six faces were obtained, characterized by precise anthropometric measurements. A text file was available for each anthropometric measure and the two genders with the numerical values for each age, from 17 to 40. A Python [31] script was written to process all the anthropometric measurements and generate a text file with the average value of each measure, considering only a specific range of years corresponding to a band.

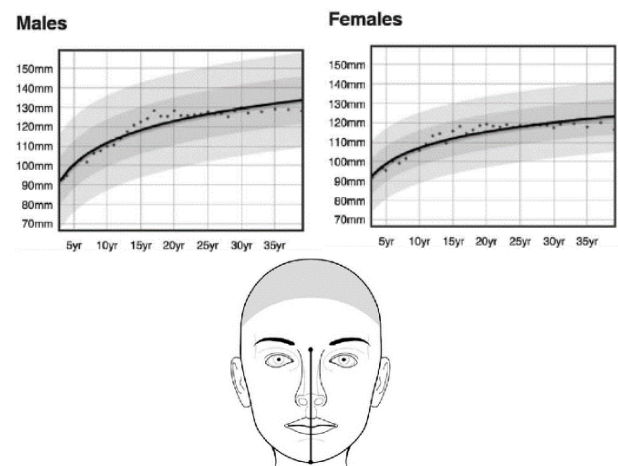


Fig. 2. Statistical trends of the distance between *nasion* and *gnation* [30].

2.2. Creation of base face in Blender

After searching for data relating to anthropometric measurements, the creation of parametric human faces started. A 3D reproduction of a volunteer's face by photogrammetry was done using well-established methodologies [32,33]. Through the VECTRA Analysis Module (VAM) software [34], the frontal and profile photos of the face were obtained. Together with the 3D face, these photos were imported in Blender and used as a reference for creating the mesh of the face.

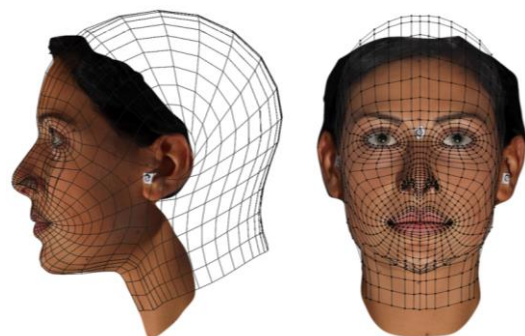


Fig. 3. Mesh creation on Blender, starting from two photos of a face

3D entities, surfaces, and volumes were created in Blender in various ways. In this work, starting from a primitive mesh (in this case, a plane), the initial mesh was enlarged by adding vertices and faces and gradually adapted to the reference face (Fig. 3), using functions available on Blender [35]. At the end of the procedure, the 3D surface (identified by a mesh) of a human face was obtained, with differences between real and virtual surfaces below 2 mm (Fig. 4).

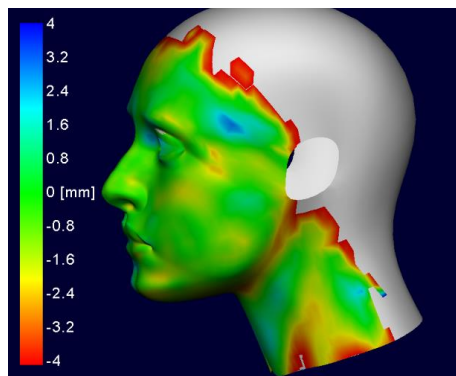


Fig. 4. Comparison of the 3D surface obtained with Blender with the 3D model obtained from the stereophotogrammetry of the same face

2.3. Parametrization of the base face

Once the basic face mesh had been obtained, a script in Python was implemented to modify the anthropometric measurements. It was possible to execute Python scripts within Blender to create or move a node, change a gradient, and automatically sequence video frames. To modify the anthropometric measurements relative to the mesh of the base face, the vertices corresponding to the classical landmarks were identified on the mesh. Each vertex was selected with the mouse, and the vertex index was extracted. This index was collected in a text file and used later to translate the relative vertex. The landmarks referred to those available in the 3DFN database, from which the values of the various anthropometric measurements were taken. Once all the indices of the vertices corresponding to the landmarks were obtained, the part of the code producing the translation of the points was written.

In the 3DFN database, some measurements are lacking, such as the angles between *nasion*, *subnasion*, *gonion*, the distance between *exocanthion* (or *endocanthion*) and the rest of the landmarks, the distances measured with the calliper, between *euryon*, *frontotemporale*, *zygion*, *gonion*, *glabella*, and *opisthocranion* and the rest of the landmarks. These problems were solved by considering this angle constant for all age groups (this assumption was not entirely correct but generated a reasonable approximation [28,32,36]) and scaling the whole face separately in the three directions. Regarding the composition of the Python code translating the vertices corresponding to the landmarks, the files relating to the anthropometric measurements were initially imported according to the gender and age range of the face to create. The scale factors were calculated, considering a scale factor for each direction (X, Y, and Z) as a fraction of representative measures calculated in the reference face and interpolated from the database. The whole face was selected and scaled in the three dimensions using these factors. The face was then rigidly

translated so that the *pronasale* coincides with the origin of the axes (0;0;0). Every single landmark was translated, comparing the current coordinates of the landmark with those calculated from the imported measurements. All translations, except the rigid ones, were proportional. Even the vertices close to the translated one, within a certain radius, were proportionally translated, thus deforming the mesh more homogeneously. In particular, a Gaussian proportionality was chosen for all the translations. Every landmark was moved individually, with a user-defined function changing the landmark of a known index of a given vector and a given radius of the zone mentioned above. The radius identifying the vertices affected by the proportional translation was set for every landmark, with an iterative process in which the result of the translation was evaluated, comparing the face visually in Blender with the original one. The entire face was rigidly translated again at the end of the procedure, as the *pronasale* might have moved from (0;0;0). A check was finally made on the correctness of the anthropometric measurements of the face obtained by printing the sizes of the obtained face on a Blender dialog box, together with those extracted from the imported file - the ideal ones. It was necessary to run the code two or three times until two measurements coincided, except for a minor error.

The following points identified the main steps of the code:

- Importing the files containing the anthropometric measurements of the face to be produced (characterized by gender and age group).
- Calculation of the scale factors for scaling the whole reference face.
- Rigid translation of the entire face to create the *pronasale* coincidence with the origin (0,0,0).
- Translations of all landmarks, following the imported anthropometric measures.
- Rigid translation of the whole face so that the *pronasale* coincides with the origin (0,0,0).
- Verification (with print on screen) of the fitting of the current anthropometric measurements with the ideal ones.

Fig. 5 and 6 show the faces of women and men (30-40 years old) due to this iterative process.



Fig. 5. Side and front view of 30-40 years old woman

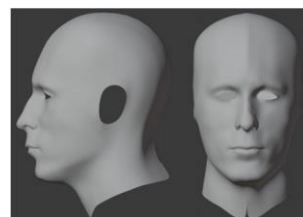


Fig. 6. Side and front view of 30-40 years old man

2.4. Evaluation of geometrical adherence for parametric faces

The assessment of the mask fit was carried out using the Geomagic software suite (3D systems Corp., Rock Hill, USA)[37]. The mask was manually aligned to the face, considering the face, the body of the mask, and the rubber (of the mask) fully rigid bodies. The movement was carried out using the *Object movement system* function in rotations and translations. This function made visible the three axes of translation and the three circumferences of rotation. By dragging an axis or a circumference, it was possible to move the object accordingly. The final position of the mask was determined to have a penetration exclusively of the rubber and not of the mask's body, searching for a continuous contact profile between the rubber and the face. Subsequently, using the *3D comparison* function, the extension of the two profiles (i.e., face and mask) was computed to interpenetrate and move apart the mask, in terms of rigid corps, excluding the deformation of the mask and the soft tissues of the face. This value could be the first indicator of the excellent fitting on the face of the mask.

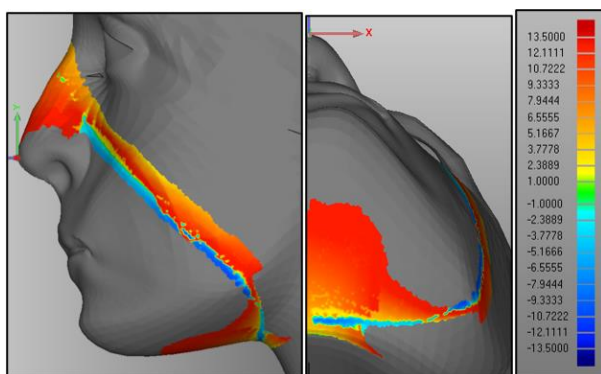


Fig. 7. Distance in millimeters of the mask from the face, the red identifies the separation, the blue the interpenetration

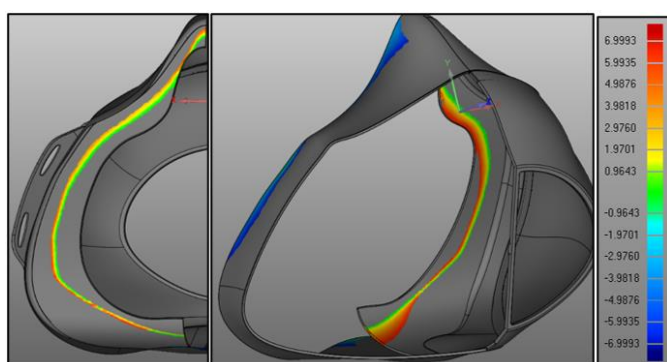


Fig. 8. Distance in millimeters of the face from the mask, red identifies both interpenetration and separation, blue the separation

The positive values (red on the color scale) were associated with separation, while the negative values (blue on the color scale) were associated with interpenetration. The null values (green on the color scale) identified the crossing points between the two profiles for all images. The results for a woman (30-40 years old) are presented in Fig. 7 and 8.

After extending the analysis to the female and male masks of the 3DFN database, the following results were achieved:

- The mask adhered well overall for male subjects if the face was not excessively thin for any age group. However, some possible discomfort could be generated as nostrils were partially pressed.
- For female faces, the mask did not rigidly and perfectly adhere to the lateral parts of the nose.
- The deformation was not considered for some female subjects because the mask could be too large.

It is important to underline again that, even if overall the mask was not fitting well, it should be considered that deformations of soft tissues and of the mask, which could lead to an improvement of the adherence, were not considered. Moreover, the mask's design used in this work was a prototype, later subjected to improvements.

3. Conclusions & future developments

3.1. Conclusions

This article presented a methodology to test the adherence of face innovative face masks, adopting a script written on Blender for generating reference faces. The faces were parametric, obtaining reference models with user-defined anthropometric measures. Using an online database of anthropometric measurements, it was possible to generate the 3D representation of many faces with an implemented script. This represented an exciting tool for designers and engineers to optimize the shape of objects that adhere to the face, such as face masks, to have the best fit considering the variety of anthropometric measures.

3.2. Future developments

This work describes a first resolution approach, neglecting the deformability of the soft tissue and of the mask. The experiments on wearability on real faces are presented in another paper, overcoming this limitation [38].

2D and 3D Finite Element Model simulations could be carried out, both considering or not the thickness of the elements. While the thickness of the mask is known, it would be necessary to obtain from the literature the mean values of thickness of soft tissues.

Another development could be to model faces for age groups from 50 years upwards and verify their adherence. Ad hoc face detections could be carried out, online databases could be used, and the reference faces modified. In addition, FEM simulations of these faces could be carried out, considering the degradation of the elasticity of the soft tissues.

Finally, it could be possible to create a simplified 1D but pseudo-3D model, to quickly simulate the interaction of the entire rubber profile that comes in contact with the face. For example, a 3D profile composed of N nodes connected by springs could model the presence of the rubber material in a simplified way. To these N nodes of the grommet, there are many N nodes as possible, which are, however, part of the face,

also connected by springs representing the soft tissues. The goal is to have a tool to quickly model and optimize any rubber pad design.

Acknowledgments

Joint research was realized in the context of R.I.A.PRO project of Politecnico di Bari (RIconversione Aziendale per la PROduzione di DPI, literally *Corporate reconversion for the PPE production*) between Politecnico di Bari and New Euroart S.r.l. (Grumo Appula, BA, Italy), who financially supported the research project.

Data from the 3D Facial Norms Database of FaceBase was used in the present work.

The authors wish to thank Mattia Lala and Roberta Corsini for their precious contributions.

References

- [1] Cucinotta D, Vanelli M. WHO Declares COVID-19 a Pandemic. *Acta Biomed* 2020;91:157–60.
- [2] Worby CJ, Chang HH. Face mask use in the general population and optimal resource allocation during the COVID-19 pandemic. *Nat Commun* 2020;11:4049.
- [3] Salmi M, Akmal JS, Pei E, Wolff J, Jaribion A, Khajavi SH. 3D printing in COVID-19: Productivity estimation of the most promising open source solutions in emergency situations. *Appl Sci* 2020;10:1–13.
- [4] Das S, Sarkar S, Das A, Das S, Chakraborty P, Sarkar J. A comprehensive review of various categories of face masks resistant to Covid-19. *Clin Epidemiol Glob Heal* 2021;12:100835.
- [5] Forouzandeh P, O'Dowd K, Pillai SC. Face masks and respirators in the fight against the COVID-19 pandemic: An overview of the standards and testing methods. *Saf Sci* 2021;133:104995.
- [6] Ju JTT, Boisvert LN, Zuo YY. Face masks against COVID-19: Standards, efficacy, testing and decontamination methods. *Adv Colloid Interface Sci* 2021;292:102435.
- [7] Liao M, Liu H, Wang X, Hu X, Huang Y, Liu X, et al. A technical review of face mask wearing in preventing respiratory COVID-19 transmission. *Curr Opin Colloid Interface Sci* 2021;52:101417.
- [8] Eikenberry SE, Mancuso M, Iboi E, Phan T, Eikenberry K, Kuang Y, et al. To mask or not to mask: Modeling the potential for face mask use by the general public to curtail the COVID-19 pandemic. *Infect Dis Model* 2020;5:293–308.
- [9] Das O, Neisiany ER, Capezza AJ, Hedenqvist MS, Försth M, Xu Q, et al. The need for fully bio-based facemasks to counter coronavirus outbreaks: A perspective. *Sci Total Environ* 2020;736:139611.
- [10] Mallakpour S, Azadi E, Hussain C. Protection, disinfection, and immunization for healthcare during the COVID-19 pandemic: Role of natural and synthetic macromolecules. *Sci Total Environ* 2021;776:145989.
- [11] Finkenzer S, Uhe T, Lavall D, Rudolph U, Falz R, Busse M, et al. Effect of surgical and FFP2/N95 face masks on cardiopulmonary exercise capacity. *Clin Res Cardiol* 2020;109:1522–30.
- [12] Tcharkhtchi A, Abbasnezhad N, Zarbini Seydani M, Zirak N, Farzaneh S, Shirinbayan M. An overview of filtration efficiency through the masks: Mechanisms of the aerosols penetration. *Bioact Mater* 2021;6:106–22.
- [13] Occupational Safety and Health Administration. OSHA Training Video Entitled Respirator Respirator Types, <<https://www.osha.gov/respiratory-protection/training>>; 2020 [accessed 15.02.2022].
- [14] Politecnico di Bari. RIAPRO - Riconversione aziendale per la produzione di DPI, <<https://www.poliba.it/it/ateneo/riaproconversione-aziendale-la-produzione-di-dpi>>; 2020 [accessed 15.02.2022].
- [15] Ufficio Stampa PoliBa. RIAPRO - Riconversione aziendale per la produzione di DPI, <<https://polibachronicle.poliba.it/riapro/>>; 2020 [accessed 15.02.2022].
- [16] New Euroart S.r.l. Lala Mask <<https://www.lalamask.it/>>; 2021 [accessed 15.02.2022].
- [17] Pedraja J, Maestre JM, Rabanal JM, Morales C, Aparicio J, Del Moral I. Role of 3D printing for the protection of surgical and critical care professionals in the COVID-19 pandemic. *Rev Esp Anestesiol Reanim* 2020;67:417–24.
- [18] Corsini L, Dammico V, Moultrie J. Frugal innovation in a crisis: the digital fabrication maker response to COVID-19. *R&D Manag* 2021;51:195–210.
- [19] Corsini L, Dammico V, Moultrie J. Critical factors for implementing open source hardware in a crisis: lessons learned from the COVID-19 pandemic. *J Open Hardw* 2020;4:8.
- [20] Ballardini R, Norrgård M, Partanen J. 3D printing, intellectual property and innovation: insight from law and technology. *Alphen aan den Rijn: Kluwer Law International*; 2017.
- [21] Stichting Blender Foundation. Blender, <<https://www.blender.org/>>; 2018 [accessed 15.02.2022].
- [22] Zomparelli A. My Face Mask Add-on Blender 2.82, <<https://www.3dwasp.com/my-face-mask-addon-blender/>>; 2020 [accessed 15.02.2022].
- [23] Trajtenberg M. A penny for your quotes: Patent citations and the value of innovations. *RAND J Econ* 1990;21:172–87.
- [24] Harhoff D, Narin F, Scherer FM, Vopel K. Citation frequency and the value of patented inventions. *Rev Econ Stat* 1999;81:511–5.
- [25] Hall B, Jaffe A, Trajtenberg M. The NBER Patent Citation Data File: Lessons, Insights and Methodological Tools. Cambridge, MA Natl Bur Econ Res 2001.
- [26] Fischer T, Henkel J. Patent trolls on markets for technology - An empirical analysis of NPEs' patent acquisitions. *Res Policy* 2012;41:1519–33.
- [27] Deli R, Di Gioia E, Galantucci LM, Percoco G. Accurate facial morphometric measurements using a 3-camera photogrammetric method. *J Craniofac Surg* 2011;22:54–9.
- [28] Galantucci LM, Percoco G, Lavecchia F. A new three-dimensional photogrammetric face scanner for the morpho-biometric 3D feature extraction applied to a massive field analysis of Italian attractive women. *Procedia - Soc Behav Sci* 2013;5:259–64.
- [29] Galantucci LM, Percoco G, Lavecchia F, Di Gioia E. Noninvasive computerized scanning method for the correlation between the facial soft and hard tissues for an integrated three-dimensional anthropometry and cephalometry. *J Craniofac Surg* 2013;24:797–804.
- [30] Samuels BD, Aho R, Brinkley JF, Bugacov A, Feingold E, Fisher S, et al. FaceBase 3: analytical tools and FAIR resources for craniofacial and dental research. *Development* 2020;147:191213.
- [31] Rossum G van. Python, <<https://www.python.org/>>; 2020 [accessed 15.02.2022].
- [32] Deli R, Galantucci LM, Laino A, D'Alessio R, Di Gioia E, Savastano C. Three-dimensional methodology for photogrammetric acquisition of the soft tissues of the face: a new clinical-instrumental protocol 2013;14:1.
- [33] Pesce M, Galantucci LM, Percoco G, Lavecchia F. A Low-cost Multi Camera 3D Scanning System for Quality Measurement of Non-static Subjects. *Procedia CIRP* 2015;28:88–93.
- [34] Canfield Scientific Inc. VAM version 2.8.3, <<https://www.canfieldsci.com/>>; 2020 [accessed 15.02.2022].
- [35] Stichting Blender Foundation. Blender 2.90 Reference Manual, <<https://docs.blender.org/manual/en/latest/index.html>>; 2020 [accessed 15.02.2022].
- [36] Galantucci LM, Deli R, Laino A, Di Gioia E, D'Alessio R, Lavecchia F, et al. Three-Dimensional Anthropometric Database of Attractive Caucasian Women: Standards and Comparisons 2016;27:1884–95.
- [37] 3D systems Corp. Geomagic, <<https://www.3dsystems.com/software/geomagic-design-x>>; 2013 [accessed 15.02.2022].
- [38] Ficarella E, Natalicchio A, Spina R, Galantucci LM. Technological scouting of bi-material face masks: experimental analysis on real faces. In: Ceretti E, Filice L, editors. *Procedia CIRP - V CIRP Conf. Biomanufacturing*, Vibo Valentia: Elsevier; 2022.
- [39] Nakamura H, Suzuki S, Kajikawa Y, Osawa M. The effect of patent family information in patent citation network analysis: a comparative case study in the drive train domain. *Scientometrics* 2015;104:437–52.